Journal of Ultrafine Grained and Nanostructured Materials
https://jufgnsm.ut.ac.ir
Vol. 57, No.1, June 2024, pp. 1-8
Print ISSN: 2423-6845 Online ISSN: 2423-6837
DOI: 10.22059/jufgnsm.2024.01.01

Effects of heat treatment on the microstructural stability, mechanical properties and degradability of as-cast Mg–1Y and Mg–1Ca alloys: A comparative study

Meysam Mohammadi–Zerankeshi, Reza Ghanbari, Reza Alizadeh*

Department of Materials Science and Engineering, Sharif University of Technology Tehran, Iran.

Recieved: 20 January 2024; Accepted: 2 February 2024

**Corresponding author email: r.alizadeh@sharif.edu*

ABSTRACT

Y and Ca are two alloying elements which are being extensively used to enhance different properties and address the challenges of biodegradable Mg alloys. In this study, the efficiency of Y and Ca for improving microstructure stability during high-temperature solution treatment was assessed and compared by studying the microstructure as well as the mechanical and degradation properties of Mg–1wt%Y and Mg–1wt%Ca alloys. X-ray diffraction and field emission scanning electron microscopy studies demonstrated presence of $Mg_{24}Y_5$ and Mg_2Ca particles in Mg–1Y and Mg–1Ca alloys, respectively. In addition, the Mg–1Y alloy witnessed a significantly higher level of grain growth in comparison with Mg–1Ca alloy. The results of shear punch test and hardness experiments demonstrated greater mechanical strength perseverance of Ca-incorporated alloy as the result of the presence of Mg_2Caphase as well as the finer microstructure. Accordingly, it can be pointed out that Ca is a more suitable element for stabilizing the microstructure of Mg-based alloys at high temperatures in comparison with Y. On the other hand, the hydrogen evolution test in phosphate-buffer saline (PBS) solution showed that Y-incorporated alloy possessed higher corrosion resistance. Also, reducing the micro-galvanic corrosion effects by long-term annealing in high temperatures can be an effective approach to enhance the degradability of both alloys, where the best corrosion resistance was observed in annealed Mg–1Y alloy.

Keywords: *Ca addition; Corrosion; Heat treatment; Mechanical properties; Thermal stability; Y addition.*

1. Introduction

Despite significant benefits of Mg alloys such as low density and high specific strength, challenges like poor stability of microstructure at high temperatures and insufficient mechanical properties as well as low corrosion resistance, restrict their wide implements [1–4]. Incorporation of alloying elements will alter the microstructure of Mg alloys in terms of grain size as well as secondary phase size, distribution and morphology. Such characteristics can be remarkably changed and controlled by utilizing heat treatment. Furthermore, it has been widely reported [5,6] that thermal stability of Mg-based alloys can be significantly improved with the addition of alloying elements [7,8]. Among different alloying elements, yttrium [9] and calcium [10] are the two mostly used elements to promote the thermal stability of Mg alloys. It is suggested that these elements can improve the microstructural stability through grain refinement and precipitation of Ca- and Y-containing particles [10]. In addition, Y and Ca can have profound effects on the corrosion resistance of Mg alloys. Subsequent heat treatment can alter the degradability of such Mg alloys [11].

In addition to microstructural stability, Ca and Y have been extensively utilized to enhance the bioperformance of Mg implants. Ca, as the main

bone component, can decrease the grain size of Mg alloys, and consequently, improve the degradation resistance and mechanical strength [12,13]. Y has been introduced as one of the interesting alloying elements for Mg alloys, where a tailored addition of Y in Mg has shown no sign of cytotoxicity, and more importantly, can significantly improve the degradation resistance by forming a Y-rich compact protective layer on the surface of the implant [14].

Ca- and Y-incorporated Mg alloys demonstrate significantly different properties in different as-cast and heat-treated conditions. In this regard, different heat treatment times and temperatures have been studied to find the optimum [1]. It has been reported [14] that heat treatment of Mg-2Ag-1Y alloy at 450 °C for 8 h can cause a significant reduction in the volume fraction of precipitates, and also lead to the formation of a uniform compact Y-rich protective corrosion film. Whereas this alloy in as-cast condition with concentrated Y element in precipitates suffered from Y depletion beneath the protective film, the existence of the Y in solution state resulted in the formation of a uniform film, which led to higher corrosion resistance [14]. Therefore, heat treatment plays an important role in controlling the microstructure and properties of such alloys.

There has been extensive research on Mg–Ca and Mg–Y alloys as biodegradable Mg alloys. Although as biodegradable implants these alloys never experience temperatures higher than 37 °C, during the fabrication steps, they might be exposed to long-term heat treatments at elevated temperatures (such as solution treatment), where the stability of microstructure and mechanical properties seems vital and can alter the properties. Accordingly, in this investigation, it was tried to compare the effect of 1 wt% addition of Y and Ca on the microstructural stability as well as the mechanical properties and corrosion behavior of Mg.

2. Materials and methods

Mg–1wt%Y and Mg–1wt%Ca alloys were cast using pure Mg, Mg-25Y master alloy and pure Ca, where details of this process is given elsewhere [15]. The chemical composition of the alloys was analyzed by employing the atomic absorption spectroscopy (AAS) test, the corresponding results of which are presented in Table 1. It can be deduced that evaluated compositions of the as-cast alloys are intimate to the nominal ones. To assess the thermal stability of alloys, samples with a protective coating to avoid oxidation, were heat treated at 400 °C for 4, 24 and 96 h, followed by a water quenching at room temperature.

The microstructure of the prepared alloys was studied by grinding and polishing with subsequent etching process a picral solution (2.5 mL acetic acid + 0.4 gr picric acid + 6 mL ethanol + 2 mL distilled water). The ImageJ software was employed to calculate the average grain size of the studied alloys, according to ASTM E112 standard. X-ray diffraction (XRD) to determine presented phases, field emission scanning electron microscopy (FESEM) as well as the energy dispersive spectroscopy (EDS) techniques for further microstructure characterization were implemented.

Vickers hardness and shear punch testing (SPT) methods were carried out to evaluate mechanical properties of the alloys. Details of the SPT technique, as a suitable approach to examine the mechanical properties of scarce materials, are given elsewhere [16]. In this method, the applied load was determined automatically as a punch displacement function, where the shear stress (τ) was calculated utilizing the below equation [17,18]:

$$\tau = \frac{P}{\pi D t} \quad (1)$$

where t is the specimen thickness, P is the punch load, D represents the average of the punch and die diameters. The mechanical experiments were car-

Table 1- The AAS test result, showing the actual chemical compositions of Mg–1Y and Mg–1Ca alloys

Alloy	Y (wt%)	Ca (wt%)	Mg
Mg–1Y	0.98	–	Balance
Mg–1Ca	–	0.99	Balance

ried out on three different specimens of each condition to ensure the validity of results.

To study the effects of Ca and Y addition on degradation behavior of Mg, in as-cast and 96-annealed conditions, hydrogen evolution test was performed. This test is believed to be an efficient and simple approach to evaluate the long-term degradability of Mg alloys [19]. For this purpose, 10 × 10 × 10 mm samples were cold-mounted and ground by 3000 grit SiC papers, followed by an immersion in phosphate buffer saline (PBS) solution at 37 ± 0.5 °C for up to 11 days. The volume of evolved hydrogen bubbles during the immersion time was calculated and plotted. To ensure the reproducibility of data, each test was conducted at least three times. Fig. 1 illustrates a schematic of the hydrogen evolution setup.

3. Results and discussion

3.1. Microstructural evolution

Fig. 2 depicts the optical microstructure of Mg–1Y and Mg–1Ca alloys in the as-cast and annealed conditions. Dendritic microstructure can be noted in as-cast alloys, which gradually disappeared with

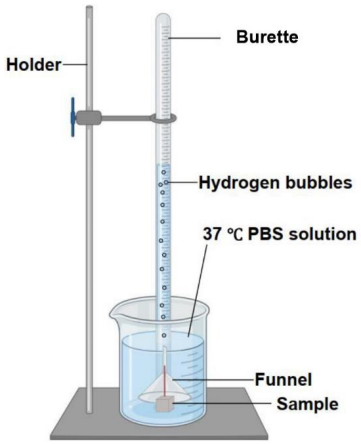

Fig. 1- Schematic illustration of the hydrogen evolution test [14].

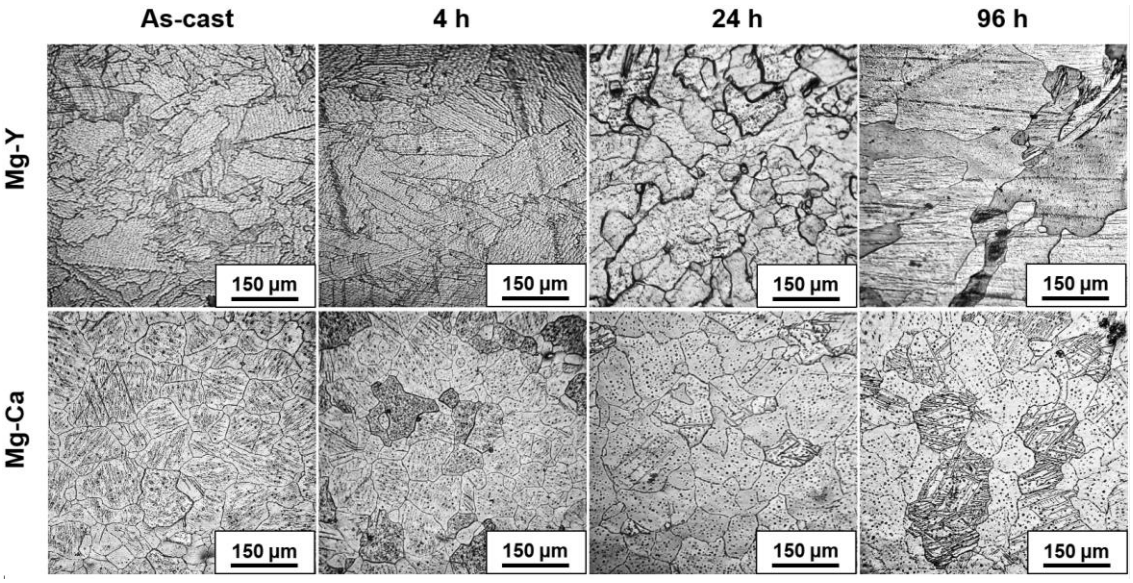

Fig. 2- Optical micrographs of the Mg–1Y and Mg–1Ca alloys in the as-cast and annealed (400 °C for 4, 24 and 96 h) conditions.

increasing the annealing time. As can be observed, the degree of grain growth is more pronounced in Y-containing alloy rather than the Ca-incorporated one, indicating the more significant influence of Ca in restricting the growth of grains. The grain size data of studied alloys in different conditions are given in Table 2. Accordingly, once Mg–1Y and Mg–1Ca alloys were annealed 96 h at 400 °C, their average grain size of increased by 199 μm and 65 μm, respectively.

Distinct behavior in thermal stability of the studied alloys can be linked to the microstructure and phase constituents of these alloys. As XRD patterns demonstrate in Fig. 3, in addition to the α-Mg peaks which present in both alloys, $Mg_{24}Y_5$ as well as Mg_2Ca phases are detected in as-cast Mg–1Y and Mg–1Ca alloys, respectively. However, while $Mg_{24}Y_5$ peaks were eliminated after annealing, indicating dissolution of this phase, the Mg_2Ca peaks were still presented in Mg–1Ca alloy, implying that this phase is stable after annealing. It has been reported that Mg_2Ca phase is the most stable compound in Mg–Ca alloys [20], and also, this phase possesses excellent thermal stability against grain coarsening [21], even superior than Mg_2Sr phase in Sr-containing Mg alloys, which are known to exhibit good microstructural stability in high temperatures [6].

In concordance with XRD analysis experiment, SEM analysis shows that in as-cast Mg–1Y alloy, some $Mg_{24}Y_5$ particles can be detected. Similarly, Ca-containing particles of Mg_2Ca are accommodated in the microstructure of Mg–1Ca alloy. As is evident, whereas secondary phases were completely dissolved after annealing at 400 °C for 96 h in Mg–1Y alloy (Fig. 4d), as was suggested in Ref [22], where all Y-containing precipitates including $Mg_{24}Y_5$ phase were dissolved in Mg-2Y alloy after heat treatment at 400 °C, a considerable number of Ca-rich particles were still remained in Ca-incorporated alloy (Fig. 4c and e). Regarding EDS analysis result exhibited in Fig. 3f, it can be suggested that Mg_2Ca phase is stable after annealing, which is the main contributor to the enhanced thermal sta-

Table 2- Grain size data of the studied alloys in the as-cast and annealed (different times) conditions

Materials	Annealing time (h)			
	0 (as-cast)	4	24	96
	Grain size (μm)			
Mg–1Y	121	134	155	320
Mg–1Ca	88	90	142	153

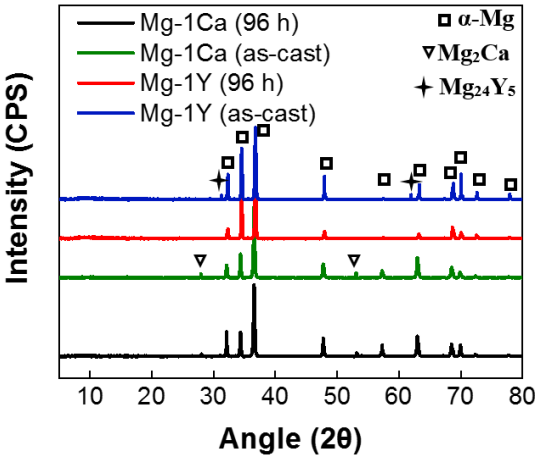

Fig. 3- XRD patterns of the Mg–1Y and Mg–1Ca alloys in as-cast and annealed (96 h at 400 °C) conditions.

bility of Mg–1Ca alloy compared to Mg–1Y alloy.

3.2. Mechanical properties

Such differences between microstructural stability of the studied alloys should be reflected in their mechanical properties. According to Fig. 5, the dissolution of precipitates as well as grain growth led to lower values of the ultimate shear strength (USS) of annealed alloys. However, Mg–1Ca alloy wit-

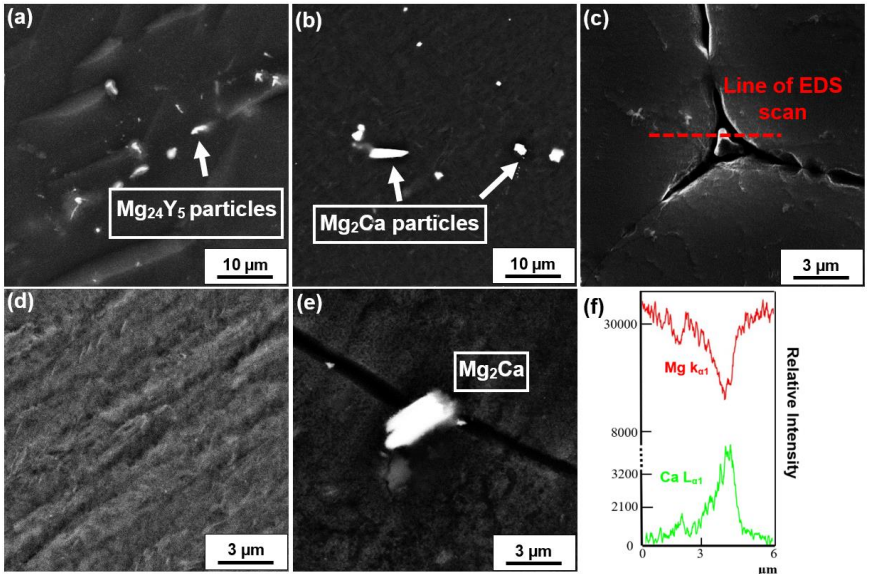

Fig. 4- FSEM micrographs of Mg–1Y (a,d) and Mg–1Ca (b,c,e) alloys in as-cast (a,b) and annealed (c,d,e) conditions, as well as the corresponding EDS line scan results of (c).

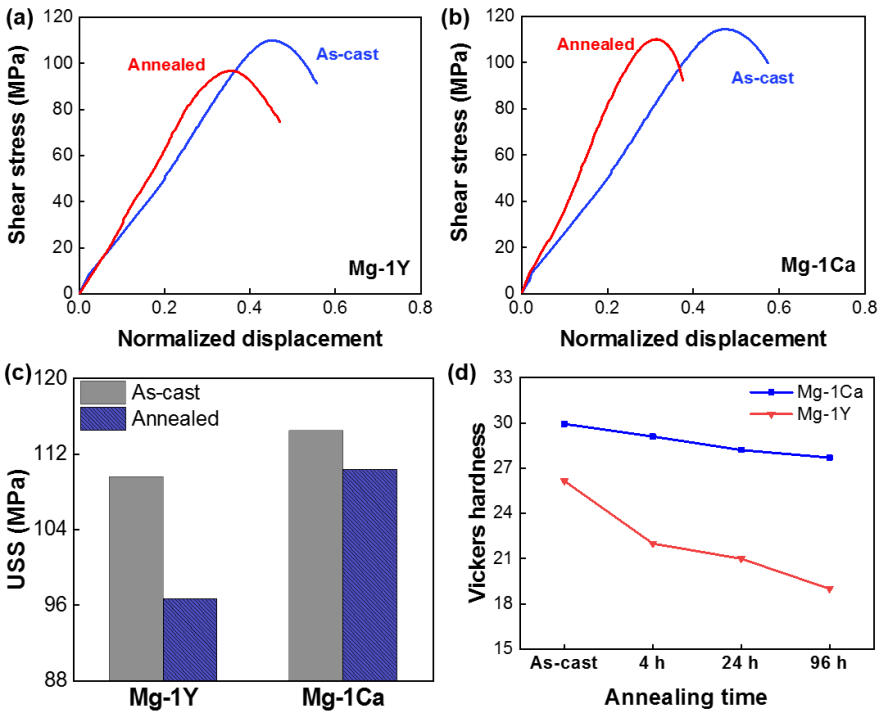

Fig. 5- SPT diagrams of Mg–1Y (a) and Mg–1Ca (b) alloys in as-cast and annealed (96 h at 400 ℃) conditions. Summary of the USS values are presented in (c). Also, variations of hardness with annealing time (at 400 ℃) are shown in (d).

nessed considerably a lower level of softening after annealing treatment in comparison with Mg–1Y alloy, where the USS value for the former decreased from 114.5 MPa to 110.4 MPa, the latter's declined from 109.6 MPa to 96.7 MPa. Furthermore, a similar trend was observed in the Vickers microhardness variation with annealing treatment time (Fig. 5d). As can be noted, the rate of hardness loss is noticeably faster in Y-containing alloy than the Ca-incorporated one. This can be attributed to the remarkable grain growth and thorough dissolution of precipitates like $Mg_{24}Y_5$ in Mg–1Y alloy. On the contrary, grain growth was less severe in Mg–1Ca alloy. Also, the Ca-rich secondary phases such as Mg_2Ca exhibited adequate stability and were not eliminated by high temperature annealing.

3.3. Degradation behavior

Hydrogen evolution test results are exhibited in Fig. 6. As can be observed, after 264 h of immersion in PBS, the Mg–1Y alloy outperformed the Mg–1Ca alloy in terms of degradation rate. Addi-

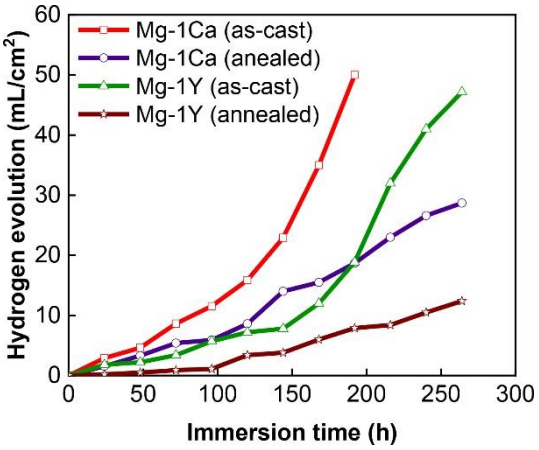

Fig. 6- Hydrogen evolution results for the investigated alloys in both as-cast and annealed (96 h at 400 °C) conditions.

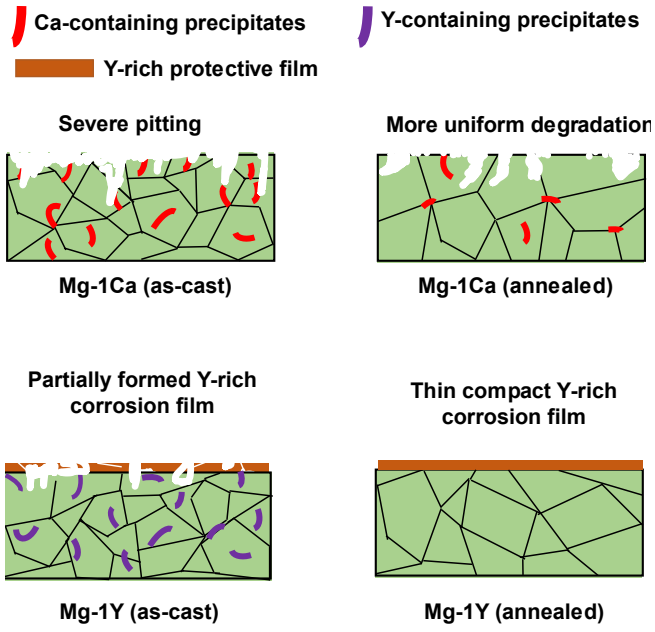

Fig. 7- Schematic illustration of the corrosion mechanism in Mg–1Ca and Mg–1Y alloys in as-cast and 96 h annealed conditions.

tionally, the annealed alloys showed significantly lower degradation rates in comparison with the as-cast materials, where the annealed Mg–1Y alloy demonstrated the best performance. Also, while a relatively stable and uniform degradation behavior can be noted in annealed alloys, the as-cast ones experienced abrupt changes in the slope of their hydrogen evolution curves, implying their higher susceptibility to corrosive medium.

Y is believed to be an effective alloying element to enhance the corrosion resistance of Mg alloys, where it can be incorporated into the corrosion film and form a protective corrosion layer [23,24]. Incorporation of 1 wt% Y in biodegradable Mg–2Ag alloy caused the formation of a thin Y-rich protective corrosion film, which remarkably improved the corrosion resistance [14]. Owing to the equal standard potential of Y with Mg, the tailored addition of Y in Mg would not cause severe micro-galvanic corrosion. On the other hand, Ca-rich secondary phases together with the dendritic microstructure of Mg–1Ca as-cast alloy led to a higher degradation rate as the result of considerable micro-galvanic corrosion between Mg matrix and Ca-containing precipitates. Dissolving such precipitates during annealing at elevated temperatures can noticeably decrease the corrosion rate [1]. In this regard, the annealed alloys suffer less from micro-galvanic corrosion, and thus, possess higher corrosion resistance. The thorough dissolution of secondary phases in Mg–1Y alloy would form a uniform Y-containing corrosion film, which is not disturbed by micro-galvanic couples and Y-depletion beneath the corrosion film. Although 96 h annealing decreased the volume fraction of secondary phases, some precipitates still existed in the annealed Mg–1Ca alloy (Fig. 4e), which can deteriorate the corrosion resistance. The corrosion mechanism of the studied alloys is schematically depicted in Fig. 7.

4. Conclusions

Thermal stability efficiency of Y and Ca, as two important alloying elements for Mg alloys, as well as their corrosion behavior were compared and following remarks were obtained:

1) $Mg_{24}Y_5$ and Mg_2Ca phases were detected in Mg–1Y and Mg–1Ca alloys, respectively. While the former dissolved by annealing at 400 °C as the result of its insufficient thermal stability, the latter remained. Accordingly, Mg–1Ca alloy showed a lower level of grain growth than Mg–1Y alloy.

2) The superior microstructural stability of Mg–1Ca alloy in comparison with Mg–1Y alloy was reflected in mechanical properties, where the Mg–1Ca alloy sustained its strength and hardness against softening during exposure to elevated temperature much better than the Mg–1Y alloy.

3) Y-incorporated Mg alloy exhibited higher corrosion resistance than Mg–1Ca alloy. Also, long-term annealing can significantly improve the degradation resistance of Mg–1Ca and Mg–1Y alloys, where the better performance of the latter can be attributed to the formation of a thin Y-rich corrosion film, which can prevent corrosion propagation.

References

1. Mohammadi Zerankeshi M, Alizadeh R, Gerashi E, Asadollahi M, Langdon TG. Effects of heat treatment on the corrosion behavior and mechanical properties of biodegradable Mg alloys. Journal of Magnesium and Alloys. 2022;10(7):1737-85.
2. Alizadeh R, Mahmudi R. Effect of Sb additions on the microstructural stability and mechanical properties of cast Mg–4Zn alloy. Materials Science and Engineering: A. 2010;527(20):5312-7.
3. Mohammadi Zerankeshi M, Alizadeh R. Ag-incorporated biodegradable Mg alloys. Materialia. 2022;23:101445.
4. O. Haghighi, Effect of steel ball diameter in the surface mechanical attrition treatment (SMAT) on microstructure, roughness, hardness and wear behavior of AZ31 magnesium alloy, J. Ultrafine Grained Nanostructured Mater. 56 (2023) 68–74.
4. Alizadeh R, Mahmudi R. Evaluating high-temperature mechanical behavior of cast Mg–4Zn–xSb magnesium alloys by shear punch testing. Materials Science and Engineering: A. 2010;527(16-17):3975-83.
6. Gerashi E, Asadollahi M, Alizadeh R, Mahmudi R. Effects of Sr additions on the microstructural stability and mechanical properties of a cast Mg–4Zn alloy. Materials Science and Engineering: A. 2022;843:143127.
7. A. Afsharnaderi, M. Lotfpour, M. Malekan, M. Emamy, Microstructural refinement and tensile properties enhancement of the Mg-9Al-1Zn alloy after hot extrusion, J. Ultrafine Grained Nanostructured Mater. 53 (2020).
8. Savaedi Z, Mirzadeh H, Aghdam RM, Mahmudi R. Effect of grain size on the mechanical properties and bio-corrosion resistance of pure magnesium. Journal of Materials Research and Technology. 2022;19:3100-9.
9. Mehrabi-Mehdiabadi M, Mahmudi R. Effects of yttrium addition on microstructural stability and elevated-temperature mechanical properties of a cast Mg–Zn alloy. Journal of Alloys and Compounds. 2020;820:153083.
10. Kondori B, Mahmudi R. Effect of Ca additions on the microstructure, thermal stability and mechanical properties of a cast AM60 magnesium alloy. Materials Science and Engineering: A. 2010;527(7-8):2014-21.
11. Ji J-H, Park I-S, Kim Y-K, Lee S-J, Bae T-S, Lee M-H. Influence of Heat Treatment on Biocorrosion and Hemocompatibility of Biodegradable Mg-35Zn-3Ca Alloy. Advances in Materials

Science and Engineering. 2015;2015:1-10.
12. Ilich JZ, Kerstetter JE. Nutrition in Bone Health Revisited: A Story Beyond Calcium. Journal of the American College of Nutrition. 2000;19(6):715-37.
13. Xie Q, Ma A, Jiang J, Liu H, Saleh B. Discharge properties of ECAP processed AZ31—Ca alloys as anodes for seawater-activated battery. Journal of Materials Research and Technology. 2021;11:1031-44.
14. Mohammadi-Zerankeshi M, Alizadeh R, Labbaf S. Improving mechanical, degradation and biological behavior of biodegradable Mg–2Ag alloy: effects of Y addition and heat treatment. Journal of Materials Research and Technology. 2023;22:1677-94.
15. Zohrevand M, Mohammadi-Zerankeshi M, Nobakht-Farin F, Alizadeh R, Mahmudi R. Degradation behavior of the as-extruded and ECAP-processed Mg–4Zn alloy by Ca addition and hydrothermal coating. Journal of Materials Research and Technology. 2022;20:1204-15.
16. Alizadeh R, Mahmudi R. Evaluating high-temperature mechanical behavior of cast Mg–4Zn–xSb magnesium alloys by shear punch testing. Materials Science and Engineering: A. 2010;527(16-17):3975-83.
17. Abdiyan F, Mahmudi R, Ghasemi HM. Effect of Mn addition on the microstructure, mechanical properties and corrosion resistance of a biodegradable Mg–Gd–Zn alloy. Materials Chemistry and Physics. 2021;271:124878.
18. Alizadeh R, Mahmudi R, Ngan AHW, Pereira PHR, Huang Y, Langdon TG. Microstructure, Texture, and Superplasticity of a Fine-Grained Mg-Gd-Zr Alloy Processed by Equal-Channel Angular Pressing. Metallurgical and Materials Transactions A. 2016;47(12):6056-69.
19. Mohammadi-Zerankeshi M, Zohrevand M, Alizadeh R. Hydrothermal Coating of the Biodegradable Mg-2Ag Alloy. Metals. 2023;13(7):1260. 20. Aljarrah M, Medraj M. Thermodynamic modelling of the Mg–Ca, Mg–Sr, Ca–Sr and Mg–Ca–Sr systems using the modified quasichemical model. Calphad. 2008;32(2):240-51.
21. Kim DH, Lee JY, Lim HK, Kyeong JS, Kim WT, Kim DH. The Effect of Microstructure Evolution on the Elevated Temperature Mechanical Properties in Mg-Sn-Ca System. MATERIALS TRANSACTIONS. 2008;49(10):2405-13.
22. Liu M, Schmutz P, Uggowitzer PJ, Song G, Atrens A. The influence of yttrium (Y) on the corrosion of Mg–Y binary alloys. Corrosion Science. 2010;52(11):3687-701.
23. Hanzi A, Gunde P, Schinhammer M, Uggowitzer P. On the biodegradation performance of an Mg–Y–RE alloy with various surface conditions in simulated body fluid. Acta Biomaterialia. 2009;5(1):162-71.
24. A. Azizi Amirabad, S.R. Allahkaram, Electrochemical behavior of nanostructured bioglass®/alginate composite coating on magnesium alloy by electrophoretic deposition for orthopedic application, J. Ultrafine Grained Nanostructured Mater. 55 (2022) 49–57.